

MPDrive: Improving Spatial Understanding with Marker-Based Prompt Learning for Autonomous Driving

Zhiyuan Zhang^{1,*}, Xiaofan Li^{2,*}, Zhihao Xu^{1,*}, Wenjie Peng¹,
Zijian Zhou³, Miaojing Shi⁴, Shuangping Huang^{1,5,†}

¹South China University of Technology, ²Baidu Inc.,
³King's College London, ⁴Tongji University, ⁵Pazhou Laboratory

Abstract

Autonomous driving visual question answering (AD-VQA) aims to answer questions related to perception, prediction, and planning based on given driving scene images, heavily relying on the model's spatial understanding capabilities. Prior works typically express spatial information through textual representations of coordinates, resulting in semantic gaps between visual coordinate representations and textual descriptions. This oversight hinders the accurate transmission of spatial information and increases the expressive burden. To address this, we propose a novel **Marker-based Prompt learning framework (MPDrive)**, which represents spatial coordinates by concise visual markers, ensuring linguistic expressive consistency and enhancing the accuracy of both visual perception and spatial expression in AD-VQA. Specifically, we create marker images by employing a detection expert to overlay object regions with numerical labels, converting complex textual coordinate generation into straightforward text-based visual marker predictions. Moreover, we fuse original and marker images as scene-level features and integrate them with detection priors to derive instance-level features. By combining these features, we construct dual-granularity visual prompts that stimulate the LLM's spatial perception capabilities. Extensive experiments on the DriveLM and CODA-LM datasets show that MPDrive achieves state-of-the-art performance, particularly in cases requiring sophisticated spatial understanding.

1. Introduction

Autonomous driving has advanced rapidly, showing potential to enhance road safety, traffic efficiency, and reduce

*These authors contribute equally.

†Corresponding Author.

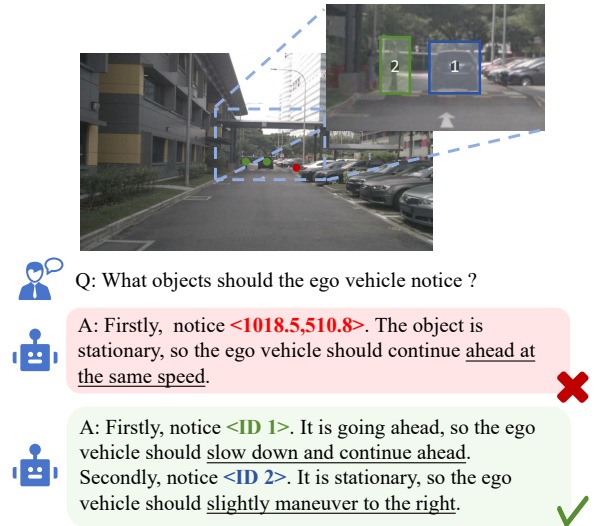


Figure 1. Comparison of object response process between main-stream MLLMs (red box) and our proposed MPDrive (green box). Current research directly represents object spatial coordinates in text format, leading to semantic gaps between coordinates and text descriptions. This misalignment adversely impacts subsequent prediction and planning tasks. In contrast, MPDrive converts complex spatial coordinate generation into text-based visual marker (region with numerical label) predictions, ensuring linguistic consistency.

human error [25, 45, 47, 52]. A robust autonomous driving system requires an agent capable of perceiving complex environments and making informed decisions. Recently, Multi-modal Large Language Models (MLLMs) have emerged as a promising approach for autonomous driving, demonstrating strong generalization capabilities in visual question answering (AD-VQA) tasks [4, 7, 18, 29, 37, 40, 48, 49, 61].

Current MLLMs face challenges in spatial understanding for autonomous driving scenarios [24, 41, 62], limit-

ing their ability to accurately locate, identify, and describe objects and their states in driving scenes. While several AD-VQA methods [19, 24, 30, 34, 39] have attempted to enhance MLLM performance through instruction tuning on domain-specific datasets, they have not adequately addressed the core challenge of spatial reasoning optimization. Among these approaches, some methods [34, 41] enhance spatial understanding by integrating detection priors. However, these methods typically express spatial coordinates in textual format, leading to inconsistencies between coordinate-based and linguistic descriptions [5, 33, 53], which undermines the perceptual accuracy and precise spatial expression in autonomous driving.

In this paper, we focus on enhancing the consistency of coordinate representations and spatial understanding in autonomous driving. We propose **Marker-Based Prompt Learning (MPDrive)**, a novel multi-modal framework that uses text indices to annotate each traffic element and directly predicts the coordinates of the corresponding index. As shown in Figure 1, MPDrive utilizes visual markers, implemented as text-based indices overlaid on detected regions in the images, to highlight the spatial location of key objects. This transformation simplifies the complex process of spatial coordinate generation into a text-based visual marker prediction, thereby bridging the gap between coordinate representations and linguistic descriptions in AD-VQA. Additionally, by incorporating multi-level spatial features, MPDrive stimulates LLM’s spatial perception capabilities to enhance the accuracy of visual marker prediction, boosting performance in predictions and planning tasks.

To this end, we propose two components: the Marker ControlNet (MCNet) and the Perception-Enhanced Spatial Prompt Learning (PSPL). Specifically, MCNet processes both the original and visual marker images, accurately expressing spatial information while preserving original image features. PSPL combines scene- and instance-level visual prompts: i) MCNet generates scene-level prompts to capture comprehensive spatial relations, while ii) instance-level prompts incorporate fine-grained object features through masked average pooling. This integration significantly enhances MPDrive’s spatial understanding capabilities.

In summary, our contributions are as follows:

- We propose MPDrive, a **Marker-based Prompt learning** framework that leverages visual markers to bridge the gap between coordinate-based and linguistic descriptions in AD-VQA, significantly improving the spatial understanding in autonomous driving.
- MPDrive consists of two components: the Marker ControlNet (MCNet) and the Perception-Enhanced Spatial Prompt Learning (PSPL). MCNet fuses visual marker images for scene features, while PSPL integrates scene- and instance-level visual prompts to enhance multi-level spa-

tial understanding.

- Extensive experiments demonstrate that MPDrive achieves state-of-the-art results on AD-VQA tasks, excelling on multi-image tasks with the DriveLM dataset [39] and single-image tasks with the CODA-LM dataset [24], particularly in complex spatial scenarios.

2. Related Work

2.1. AD-VQA

AD-VQA has emerged as an essential component for promoting human-vehicle interaction and improving decision-making in complex driving scenarios [55]. Recent autonomous driving research has advanced through multiple perspectives: multi-modal fusion for scene understanding [37], multi-step reasoning for decision-making [39, 44], signal control optimization [15], motion planning [31], and corner-case handling [24]. These approaches collectively enhance the system’s capabilities through effective integration of multi-modal data and reasoning mechanisms.

Recent research has increasingly focused on enhancing the spatial understanding capabilities of MLLMs in autonomous driving. ELM [61] leverages expert-generated textual descriptions to improve object localization, while LLM-Driver [4] advances context understanding by integrating vectorized numeric modalities with pre-trained LLMs. Similarly, Reason2Drive [34] employs a prior tokenizer and an instructed vision decoder to strengthen visual localization capabilities. Although these strategies aim to enhance spatial understanding through detection priors, they often involve complex training schemes, such as the addition of intricate network architectures or detection optimization functions. Furthermore, these strategies typically represent spatial coordinates in text format, which may increase the complexity of the model. Consequently, these approaches neglect the discrepancies between coordinate-based and linguistic descriptions, which compromises perceptual accuracy and the precise articulation of spatial information in autonomous driving systems.

2.2. MLLMs

MLLMs have demonstrated remarkable interpretability and generalization capabilities [18, 33, 50]. Recent advances in MLLMs primarily focus on vision-language alignment and training strategies. For alignment, BLIP-2 [23] introduces Q-Former for efficient modality bridging, MiniGPT-4 [62] aligns frozen visual encoders with LLMs through projection layers, and InternVL [6] proposes progressive alignment between vision models and LLMs. For training strategies, LLAVA [27] utilizes machine-generated instruction data, while MiniCPM [17] optimizes performance through advanced learning rate scheduling. These advances have enabled MLLMs’ successful applications in video un-

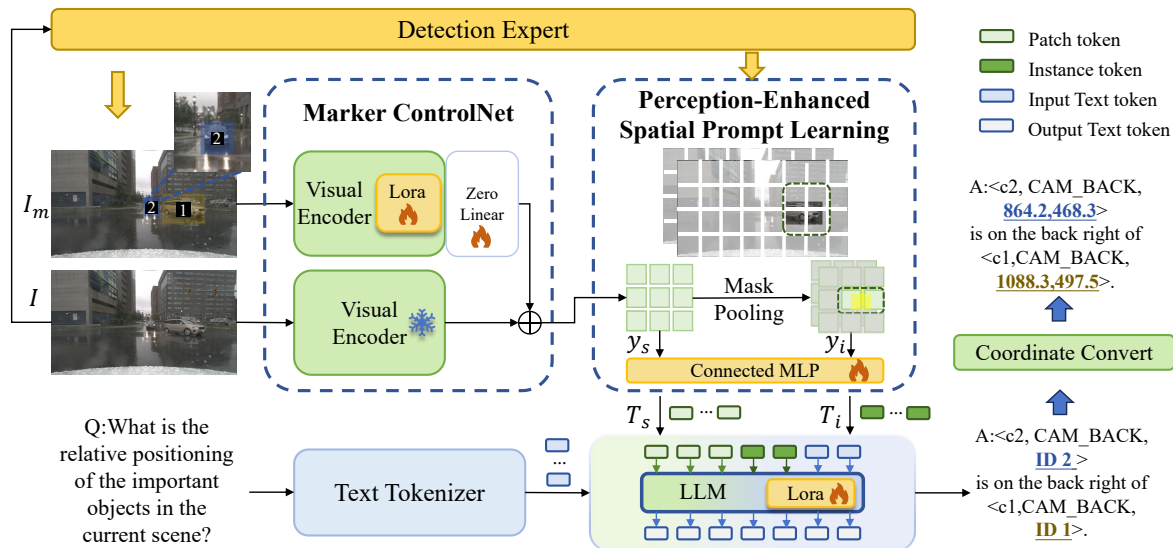


Figure 2. Overview of the MPDrive framework. For clarity, we illustrate the process using a single-view image. The detection expert generates a visual marker image I_m . This marker image I_m and the original image I are processed by MCNet to extract scene-level features y_s . For the Perception-Enhanced Spatial Prompt Learning module, these scene-level features y_s undergo mask average pooling for each instance mask to obtain instance-level features y_i . Subsequently, both scene-level features y_s and instance-level features y_i are processed through a connected MLP to generate visual prompts T_s and T_i respectively. Finally, these visual prompts, combined with text embeddings, are fed into the Large Language Model to generate the output \hat{s} . For coordinate prediction, MPDrive predicts the marker index k corresponding to the target object and then converts it into the respective coordinates.

derstanding [32, 51], image understanding [8, 9, 12, 22, 36], and embodied AI [10, 57].

In autonomous driving, MLLMs have been explored in various ways. Atlas [2] and DriveGPT4 [49] enhance driving capabilities through 3D tokenization and multi-frame video processing, respectively. For resource efficiency, MiniDrive [58] and EM-VLM4AD [14] provide lightweight MLLMs for autonomous driving. Meanwhile, TOKEN [40] integrates tokenized object-level knowledge, while DriveAdapter [21] improves model performance through feature alignment and action-guided learning. These efforts attempt to apply MLLMs in autonomous driving; however, they have not sufficiently explored spatial understanding in driving scenarios.

2.3. Visual Prompts

Visual prompts have been extensively used for transfer and adaptation across various downstream tasks [11, 20, 46, 60] and can be categorized into learnable and image-modifying approaches. Learnable visual prompt methods incorporate trainable tokens as additional visual inputs [13, 20, 38], with works like LM-BFF [13] and VPT [20] demonstrating enhanced learning efficiency through prompt-based fine-tuning. Image-modifying visual prompt methods focus on altering images with expert-generated elements [53, 54, 56], where FGVP [54], API [56], and SoM [53] have shown

significant improvements in MLLMs’ visual understanding through techniques such as segmentation masks and attention heatmaps.

While our approach draws inspiration from SoM [53], which overlays masks and markers on images, we have introduced several key improvements to better address the specific challenges in autonomous driving tasks. First, conventional markers may obscure critical information in the original image, such as object colors and features. To address this, we employ Marker ControlNet to introduce visual markers that gradually incorporate marker-derived information, thereby preserving key visual information from the original image while leveraging the benefits of visual markers. Additionally, we incorporate a visual prompt process: Perception-Enhanced Spatial Prompt Learning, which includes scene-level and instance-level visual prompts, significantly enhancing the spatial perception capabilities of MPDrive.

3. Method

This section is organized as follows. Section 3.1 introduces the preliminary knowledge, including the task definition and MLLM pipeline. Section 3.2 details the Visual Marker. Section 3.3 presents two core modules of MPDrive: Marker ControlNet (MCNet) and Perception-

Enhanced Spatial Prompt Learning (PSPL).

3.1. Preliminary

Given a set of m view images $\{I_1, I_2, \dots, I_m\}$ and a text question Q , AD-VQA aims to generate a response sequence $\hat{S} = (\hat{s}_1, \hat{s}_2, \dots, \hat{s}_N)$, where \hat{s}_i denotes the i -th token in the sequence of length N . The workflow of MLLMs in AD-VQA is as follows: 1) a visual encoder that extracts visual features from each view I_i ; 2) a connected MLP that transforms multi-view features into image tokens; 3) a text tokenizer that converts the question Q into text tokens; and 4) an LLM that fuses image tokens and text tokens to generate the response sequence \hat{S} .

Building upon these MLLMs, we propose MPDrive to enhance spatial understanding capabilities. For clarity, we illustrate the methodology using a single-view scenario, while noting that all operations naturally extend to multi-view cases.

3.2. Visual Marker

To bridge the gap between spatial coordinate representations and linguistic descriptions, we introduce Visual Marker. This approach simplifies the task of spatial coordinate generation by converting it into straightforward text-based visual marker predictions. As illustrated in Figure 2, given an input image $I \in \mathbb{R}^{H \times W \times 3}$, we use a detection expert, StreamPETR [43], to identify traffic objects (*e.g.*, cars, trucks, and buses), following the object categories specified in [43]. The detection expert generates K object masks, represented as binary masks $R = [r_1, r_2, \dots, r_K]$, where $r_k \in \{0, 1\}^{H \times W}$ denotes the k -th detection mask. For r_k , we compute its average centroid coordinates $c_k = (x_k, y_k)$, which represents the central location of this object. The annotated marker image I_m is generated by modifying the original image I through two steps: First, annotating the marker index k at each object’s centroid $c_k = (x_k, y_k)$, and second, overlaying corresponding semi-transparent mask regions r_k to describe object boundaries. Furthermore, when new spatial coordinates c_{new} (more than d_{th} pixels from existing coordinates) are referenced in the question Q , we assign them a marker index $K+1$ and annotate the index on I_m to maintain consistent spatial reasoning across visual and text modalities.

For response generation, we leverage the Visual Marker to improve the effectiveness of visual prompts and ensure consistency of language output. Specifically, the LLM first generates the indicator k from the given images and the question, then maps this index k to its corresponding centroid coordinates $c_k = (x_k, y_k)$ for precise localization. This process allows MPDrive to identify the key objects by their markers, while complex spatial perception is handled by the Detection Expert. By avoiding direct coordinate output, this approach mitigates the linguistic complexity for

LLMs, ensuring consistent text output.

3.3. MPDrive Architecture

As illustrated in Figure 2, MPDrive consists of two key components: MCNet and PSPL. MCNet enhances spatial representation by leveraging both the original image and the additional visual marker image to achieve dual-level fused scene features. Based on these extracted features and the detection expert, PSPL generates scene-level and instance-level visual prompts, thereby enhancing the understanding of driving scene information and object information. The integration of these components significantly boosts the spatial perception capabilities of MPDrive.

Marker ControlNet. To effectively preserve key features of the original image and fully leverage the rich information in visual markers, we propose the Marker ControlNet (MCNet). This module takes both the original image and the visual marker image as input, and generates scene-level features.

We freeze the parameters θ of the original visual encoder E and create a trainable copy with parameters θ_c , denoted as E_c . During training, the original visual encoder remains frozen, and we focus on training the new control block using Low-Rank Adaptation (LoRA) [16] on the multi-head attention modules and the feed-forward networks with the rank of 16. We connect the original visual encoder and the control block with a zero linear, Z , where both weight and bias are initialized to zero, with parameters θ_z . These layers are trained alongside the control block, allowing for effective parameter tuning and improved performance. The original image features are extracted using the original visual encoder E , while the visual marker image features are extracted using the new control block, E_c combined with Z . These features are combined through element-wise addition for scene-level feature fusion:

$$y_s = E(I; \theta) + Z(E_c(I_m; \theta_c); \theta_z), \quad (1)$$

where y_s represents the scene-level features.

Since the weight and bias parameters of the zero linear layer are initialized to zero, the Z term in Equation 1 starts with zero, thereby preserving the integrity of the original image features. During subsequent optimization phases, beneficial features from the visual marker image will be gradually introduced through backpropagation.

MCNet effectively incorporates visual markers, enabling MPDrive to learn additional semantic information through the guidance of visual markers while preserving the critical features of the original image. More importantly, this approach ensures that MPDrive can capture the visual marker information and then output the corresponding text-based markers, thereby maintaining consistency in linguistic output when generating spatial information.

Perception-Enhanced Spatial Prompt Learning. To address the limitations of MLLMs in spatial expression capabilities, we introduce Perception-Enhanced Spatial Prompt Learning (PSPL), aiming at enhancing the spatial perception of MPDrive by utilizing both scene-level and instance-level visual prompts.

Visual markers in images accurately represent the spatial information for the entire scene. Therefore, the output features y_s of MCNet encompass rich scene-level spatial information. Subsequently, y_s is processed through the connected MLP to generate scene-level visual prompts T_s . These scene-level visual prompts significantly improve the perception and accurate understanding of spatial information in complex scenarios.

To further enhance the representation of spatial information at the instance level, we introduce instance-level visual prompts. Given the k -th detection object with its region mask r_k , the scene-level visual prompts $y_s \in \mathbb{R}^{H' \times W' \times C}$, where C is the number of channels, W' is the width, and H' is the height, we resize the binary region mask r_k into the same size as y_s and use mask average pooling:

$$y_i^k = \text{MAP}(y_s, r_k), \quad (2)$$

where MAP represents the mask average pooling operation, and y_i^k denotes the k -th instance-level visual features.

Given K objects, we obtain a set of instance-level visual features $\{y_i^1, \dots, y_i^K\}$. These features are processed through a Connected MLP to generate instance-level visual prompts T_i . This instance-level visual prompts enriches object spatial representation. PSPL concatenates the scene-level visual prompts T_s and the instance-level visual prompts T_i together, enhancing the spatial perception ability of MPDrive.

Large Language Model. The LLM receives input text tokens from the text tokenizer and spatial prompts T_s and T_i from the PSPL module. It processes these inputs using its internal model, where LoRA is applied to both multi-head attention modules and feed-forward networks at a rank of 16, generating an output sequence $\hat{S} = (\hat{s}_1, \hat{s}_2, \dots, \hat{s}_N)$ of N words. The output token sequence \hat{S} is then used to compute cross-entropy loss with the ground truth sequence $S = (s_1, s_2, \dots, s_N)$:

$$\text{Loss} = - \sum_{i=1}^n s_i \log(\hat{s}_i). \quad (3)$$

4. Experiments

In this section, we comprehensively evaluate the efficacy of MPDrive. Section 4.1 introduces the experimental setup, while Section 4.2 and Section 4.3 provide an in-depth analysis of the quantitative and qualitative results. Lastly, Sec-

tion 4.4 presents ablation studies to evaluate the contribution of each component.

4.1. Experimental Setting

Datasets. We conduct experiments on the DriveLM [39] and CODA-LM [24] datasets. For the DriveLM dataset, we follow the data partitioning strategy employed by EM-VLM4AD [14] and MiniDrive [58], which divides the dataset into training and validation subsets, allocating 70% and 30% of the data, respectively. The training set comprises 341,353 unique QA pairs, while the validation set contains 18,817 distinct QA pairs. Each QA pair consists of six view images: front view, left front view, right front view, back view, left back view, and right back view. For the CODA-LM dataset, we train MPDrive using a training set of 20,495 QA pairs and validate it with a mini set of 193 QA pairs. Each QA pair consists of a front-view image.

Evaluation Metrics. To facilitate a rigorous and fair comparison, we adopt the evaluation metrics consistent with those used in EM-VLM4AD and MiniDrive studies, including the BLEU-4 [35], ROUGE-L [26], CIDEr [42], and METEOR [3]. These metrics evaluate the linguistic consistency between predicted values and ground truth through overlap, recall, consensus-based evaluation, and semantic similarity, reflecting the perception, prediction, and planning capabilities of MLLMs. Additionally, following the CVPR 2024 Autonomous Driving Challenge guidelines [39, 61], we incorporate additional performance metrics: match and accuracy. The match metric quantifies the percentage of predicted center point coordinates that have an Euclidean distance of less than 16 pixels from the ground truth, providing an intuitive validation of the spatial information expression capabilities of MLLMs. Accuracy evaluates the correctness of responses in multiple-choice and yes/no questions, offering a comprehensive assessment of MLLMs' capabilities.

Implementation Details. During the training phase, we employ a cosine learning schedule with an initial rate of $5e - 4$ and utilize the AdamW [28] optimizer with a weight decay of 0.01. For the DriveLM dataset, we employ a batch size of 128 and conducted training for 3,000 iterations across eight A800 GPUs, equivalent to approximately 1 epoch. For the CODA-LM dataset, we conducted training for 2000 iterations, equivalent to approximately 12 epochs. Throughout the entire training process, the visual encoder weights remained frozen. We fine-tune the connected MLP and zero MLP while applying Low-Rank Adaptation (LoRA) [16] to both the visual encoder within MCNet and the LLM decoder. For both the training and inference stages, we resize the input image resolution to 448×448 pixels. The number of detected objects K is dynamically determined by the detection expert for each image, with a maximum limit of 100 objects across all camera

Method	Inference Schema	Spatial↑ Perception	Language↑				
		Match	Accuracy	BLEU-4	ROUGE_L	CIDEr	METEOR
DriveLM-Agent [39]	Graph	-	-	53.09	66.79	2.79	36.19
EM-VLM4AD [14]	Single	-	-	45.36	71.98	3.20	34.49
MiniDrive [58]	Single	-	-	50.20	73.50	3.32	<u>37.40</u>
LLaMA-Adapter [59]	Single	1.48	66.66	45.96	69.78	3.07	33.66
InternVL-2 [6]	Single	<u>7.59</u>	<u>82.54</u>	51.42	77.08	<u>3.53</u>	37.12
Ours: MPDrive	Single	13.43	85.18	<u>52.71</u>	<u>76.98</u>	3.56	38.31

Table 1. Quantitative evaluation on the DriveLM dataset. MPDrive significantly outperforms existing approaches in both spatial perception and language understanding metrics. **Bold** indicates the highest value, while an underline indicates the second-highest value.

Method	General↑	Regional Perception↑						Suggestion↑
	Text-Score	ALL	Vehicle	VRU	Cone	Barrier	Other	Text-Score
LLaVA1.5 [27]	22.60	34.78	40.00	28.00	32.22	24.00	10.00	14.20
Qwen-VL-Chat [1]	26.00	53.33	57.76	<u>60.00</u>	48.89	44.29	35.71	35.40
Qwen-VL-Max [1]	<u>34.60</u>	<u>68.17</u>	<u>69.83</u>	56.00	<u>80.00</u>	59.29	65.71	<u>47.40</u>
MiniDrive [58]	24.60	66.34	67.41	36.00	84.44	<u>62.86</u>	<u>62.85</u>	45.44
Ours: MPDrive	41.80	76.12	79.48	70.00	77.77	70.00	<u>62.85</u>	58.20

Table 2. Quantitative evaluation on the CODA-LM dataset. MPDrive achieves superior performance across all evaluation metrics. **Bold** indicates the highest value, while an underline indicates the second-highest value.

views. We set new spatial coordinates $d_{th} = 50$.

4.2. Quantitative Results

We conduct the quantitative evaluation with competitive methods on the DriveLM dataset to demonstrate the effectiveness of MPDrive, as shown in Table 1. Our proposed method demonstrates outstanding performance, particularly in the CIDEr and METEOR metrics, achieving scores of 3.56 and 38.31, respectively. Furthermore, it outperforms all single-turn inference approaches in BLEU-4, closely approximating the performance of the graph-based multi-turn reasoning method (DriveLM-Agent), indicating its superior performance in linguistic consistency. Additionally, MPDrive demonstrates strong spatial perception abilities with a match score of 13.43 and an accuracy of 85.18, which surpasses the performance of InternVL-2.

As shown in Table 2, MPDrive demonstrates remarkable performance across various tasks on the CODA-LM dataset. In the general perception task, MPDrive achieves a score of 41.80, significantly outperforming other competitive methods. This indicates its superior ability to perceive and interpret driving scenes effectively. For the spatially relevant region perception task, MPDrive excels in several subcategories. It achieves a score of 79.48 in the vehicle category and 70.00 in the VRU (Vulnerable Road Users) category, underscoring its fine-grained perception capabilities for spatial objects. Additionally, it performs well in the cone (77.77), barrier (70.00), and other (62.85) categories, highlighting its comprehensive spatial understanding. MPDrive

achieves a top score of 58.20 in driving suggestion generation, demonstrating superior spatial awareness and planning capabilities for effective driving recommendations.

These results validate MPDrive for precise spatial expression and demonstrate MPDrive’s enhanced spatial perception capabilities in autonomous driving scenarios.

4.3. Qualitative Examples

In Figure 3, we compare the actual response results of MPDrive with InternVL-2 on unseen samples, evaluating the spatial perception and the task planning capabilities of MPDrive. In the upper sample of Figure 3, we display the predicted coordinates from one of the most relevant images. The predictions of InternVL-2 are located in incorrect areas, while MPDrive locates the important objects, aligning with ground truth annotations. This demonstrates superior spatial understanding capabilities of MPDrive.

In the lower example of Figure 3, when asked to identify dangerous behaviors involving vehicles and pedestrians, InternVL-2 incorrectly concludes no collision risk with the pedestrian. In contrast, MPDrive accurately assesses the vehicle-pedestrian spatial relationship, leading to correct planning decisions. This demonstrates the advanced ability of MPDrive to analyze complex scenarios and make precise decisions, highlighting its effectiveness in autonomous driving applications. More qualitative examples can be found in the supplementary materials.

In conclusion, MPDrive outperforms InternVL-2 on unseen samples, exhibiting accurate object localization and re-

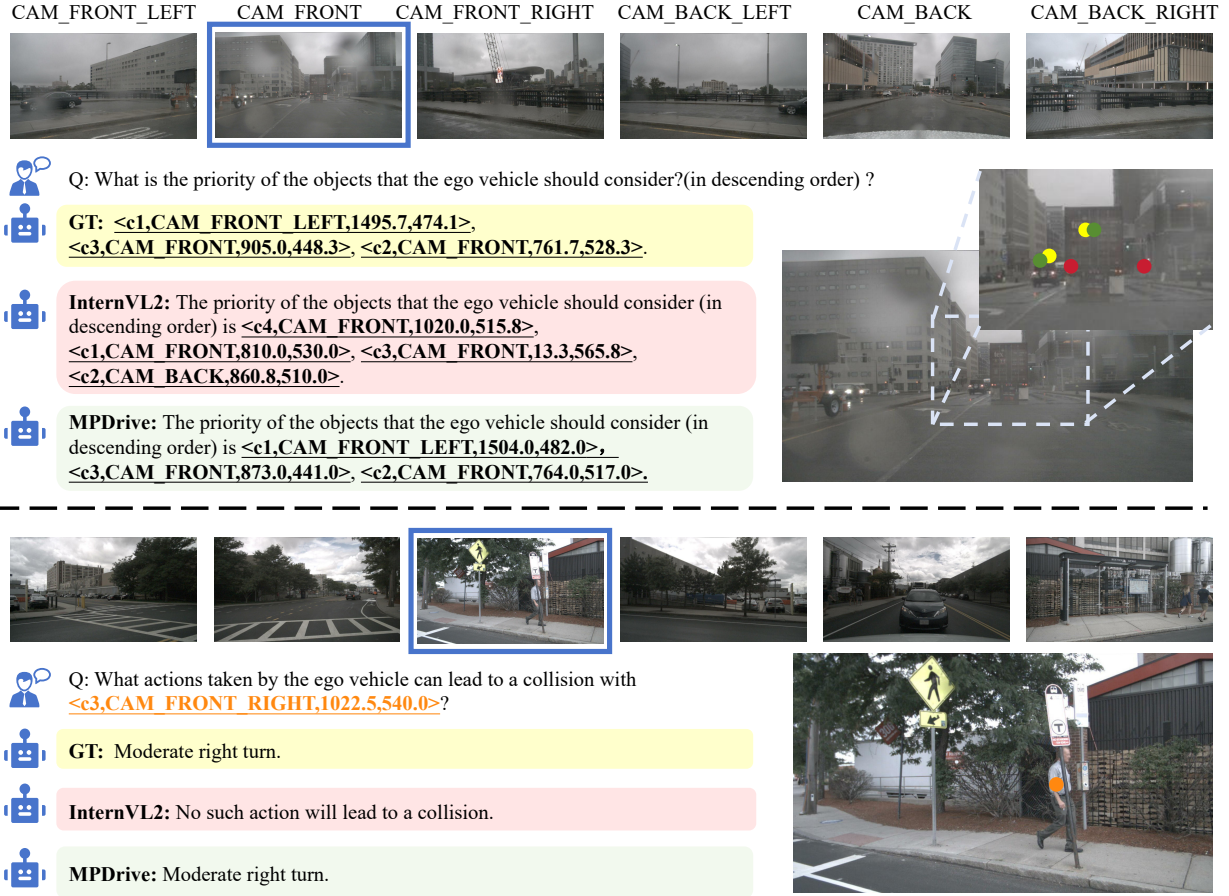


Figure 3. Comparison of the responses between InternVL-2 and our proposed MPDrive. The yellow (■) area and dots represent the response and coordinates of ground truth (GT), the green (■) area and dots indicate the response and coordinates of MPDrive, the red (■) area and dots denote the response and coordinates of InternVL-2. The blue box (□) indicates the image that is most relevant to the response, with an enlarged version of this image located in the bottom right corner of each sample, the orange dots (●) represent the positions of the coordinates in the image related to the question.

liable assessment of spatial relations, which are crucial for safe autonomous driving.

4.4. Ablation Studies

In this section, we conduct ablation studies on visual markers, MCNet, and instance-level visual prompts. Furthermore, we evaluate MPDrive across different MLLMs. To ensure a fair comparison, we conducted ablation experiments on the DriveLM dataset [39], which includes six-view images and encompasses perception, prediction, and planning tasks, thereby facilitating a comprehensive assessment of MLLM in autonomous driving scenarios. Furthermore, the various evaluation metrics on the DriveLM dataset can evaluate the performance of MPDrive from multiple perspectives.

Scene-level Visual Prompts. To evaluate the effectiveness of the scene-level visual prompts, we conduct ablation experiments for Visual Marker and MCNet. Table 3

presents the ablation study of scene-level prompts. Visual marker significantly improves spatial perception, as seen in the match score from 7.59 to 11.89. However, its impact on language metrics shows mixed results. While the accuracy slightly decreases to 80.42, the improvements in BLEU-4 and METEOR scores indicate enhanced linguistic expression consistency in MPDrive. We attribute this performance to the potential feature interference between Visual Markers and object features in the visual space.

By incorporating the MCNet, most metrics for measuring language consistency have improved. While the match score decreases from 11.89 to 9.70 compared to using Visual Marker alone, the model achieves better linguistic quality with improved BLEU-4 (52.56) and METEOR (38.14) scores. This suggests that MCNet helps balance the feature representation between spatial information and semantic understanding, though at the cost of some spatial perception capability.

Scene-level Visual Prompts		Instance-level Visual Prompts	Spatial↑ Perception	Language↑				
Visual Marker	MCNet		Match	Accuracy	BLEU-4	ROUGE_L	CIDEr	METEOR
-	-	-	7.59	<u>82.54</u>	51.42	77.08	<u>3.53</u>	37.12
✓	-	-	<u>11.89</u>	80.42	52.04	76.17	3.50	37.88
✓	✓	-	9.70	78.83	<u>52.56</u>	76.53	<u>3.53</u>	<u>38.14</u>
✓	✓	✓	13.43	85.18	52.71	<u>76.98</u>	3.56	38.31

Table 3. Ablation experiments on different parts of MPDrive on the DriveLM dataset. **Bold** indicates the highest value, while an underline indicates the second-highest value.

Method	MPDrive	Spatial↑ Perception	Language↑				
		Match	Accuracy	BLEU-4	ROUGE_L	CIDEr	METEOR
LLaMA-Adapter [59]	-	1.48	66.66	45.96	69.78	3.07	33.66
	✓	<u>10.05</u>	68.25	47.97	73.54	3.28	35.58
InternVL-2 [6]	-	7.59	<u>82.54</u>	<u>51.42</u>	77.08	<u>3.53</u>	<u>37.12</u>
	✓	13.43	85.18	52.71	<u>76.98</u>	3.56	38.31

Table 4. Ablation studies of MPDrive using different MLLMs on the DriveLM dataset. MPDrive significantly enhances the spatial understanding performance of MLLMs. **Bold** indicates the highest value, while an underline indicates the second-highest value.

Instance-level Visual Prompts. To evaluate the effectiveness of the instance-level visual prompts, we conduct comparative experiments with and without this component while keeping all other settings identical, as shown in Table 3. The integration of instance-level visual prompts leads to comprehensive improvements across both spatial and language metrics. Specifically, the match score further increases to 13.43, surpassing all previous configurations, while the accuracy achieves the highest value of 85.18. Moreover, the language generation quality consistently improves, with BLEU-4 reaching 52.71, ROUGE_L at 76.98, CIDEr at 3.56, and METEOR achieving 38.31. These results demonstrate that the instance-level visual prompts effectively enhance both spatial perception and language understanding, suggesting its crucial role in precise text-based marker index prediction.

Different MLLMs. To assess the model-agnostic nature of MPDrive, we extend our experiments to include LLaMA-Adapter as an alternative MLLM. Table 4 demonstrates that applying our MPDrive framework to LLaMA-Adapter yields significant performance gains compared to the original LLaMA-Adapter implementation. Specifically, MPDrive (LLaMA-Adapter) achieves a significantly higher match score of 10.05 compared to LLaMA-Adapter’s 1.48, indicating a substantial enhancement in spatial perception capabilities. In terms of language generation metrics, MPDrive (LLaMA-Adapter) outperforms LLaMA-Adapter in all aspects: BLEU-4 increases from 45.96 to 47.97, ROUGE-L improves from 69.78 to 73.54, CIDEr rises from 3.07 to 3.28, and METEOR advances from 33.66 to 35.58. Additionally, MPDrive demonstrates slightly higher Accu-

racy at 68.25 compared to 66.66. The comparative analysis indicates that MPDrive effectively enhances the spatial understanding of different MLLMs.

5. Conclusion

We introduce a novel MLLM-based framework called MPDrive for AD-VQA. MPDrive transforms complex spatial coordinate generation into concise visual marker predictions. It incorporates MCNet and PSPL to enhance both scene-level and instance-level spatial perception capabilities. MPDrive achieves state-of-the-art performance on the multi-view input autonomous driving task with the DriveLM dataset, as well as on the single-view input task with the CODA-LM dataset.

MPDrive relies on a prior expert for spatial perception and language expression, and errors from the expert can affect its performance. Furthermore, although MPDrive enhances the spatial perception capabilities of AD-VQA, the long-horizon temporal perception remains a significant challenge in autonomous driving. Therefore, exploring how to advance this research based on MPDrive is worthy of further investigation.

References

- [1] Jinze Bai, Shuai Bai, Yunfei Chu, Zeyu Cui, Kai Dang, Xiaodong Deng, Yang Fan, Wenbin Ge, Yu Han, Fei Huang, Binyuan Hui, Luo Ji, Mei Li, Junyang Lin, Runji Lin, Dayiheng Liu, Gao Liu, Chengqiang Lu, Keming Lu, Jianxin Ma, Rui Men, Xingzhang Ren, Xuancheng Ren, Chuanqi Tan, Sinan Tan, Jianhong Tu, Peng Wang, Shijie Wang, Wei Wang, Shengguang Wu, Benfeng Xu, Jin Xu, An Yang,

- Hao Yang, Jian Yang, Shusheng Yang, Yang Yao, Bowen Yu, Hongyi Yuan, Zheng Yuan, Jianwei Zhang, Xingxuan Zhang, Yichang Zhang, Zhenru Zhang, Chang Zhou, Jingren Zhou, Xiaohuan Zhou, and Tianhang Zhu. Qwen technical report. *arXiv preprint arXiv:2309.16609*, 2023. 6
- [2] Yifan Bai, Dongming Wu, Yingfei Liu, Fan Jia, Weixin Mao, Ziheng Zhang, Yucheng Zhao, Jianbing Shen, Xing Wei, Tiancai Wang, and Xiangyu Zhang. Is a 3d-tokenized LLM the key to reliable autonomous driving? *CoRR*, abs/2405.18361, 2024. 3
- [3] Satanjeev Banerjee and Alon Lavie. METEOR: an automatic metric for MT evaluation with improved correlation with human judgments. In *ACL Workshop*, pages 65–72, 2005. 5
- [4] Long Chen, Oleg Sinavski, Jan Hünermann, Alice Karnsund, Andrew James Willmott, Danny Birch, Daniel Maund, and Jamie Shotton. Driving with llms: Fusing object-level vector modality for explainable autonomous driving. In *ICRA*, pages 14093–14100, 2024. 1, 2
- [5] Ting Chen, Saurabh Saxena, Lala Li, David J. Fleet, and Geoffrey E. Hinton. Pix2seq: A language modeling framework for object detection. In *ICLR*, 2022. 2
- [6] Zhe Chen, Jiannan Wu, Wenhai Wang, Weijie Su, Guo Chen, Sen Xing, Muyan Zhong, Qinglong Zhang, Xizhou Zhu, Lewei Lu, Bin Li, Ping Luo, Tong Lu, Yu Qiao, and Jifeng Dai. Internvl: Scaling up vision foundation models and aligning for generic visual-linguistic tasks. *CoRR*, abs/2312.14238, 2023. 2, 6, 8
- [7] Tushar Choudhary, Vikrant Dewangan, Shivam Chandhok, Shubham Priyadarshan, Anushka Jain, Arun K. Singh, Siddharth Srivastava, Krishna Murthy Jatavallabhula, and K. Madhava Krishna. Talk2bev: Language-enhanced bird’s-eye view maps for autonomous driving. In *ICRA*, pages 16345–16352, 2024. 1
- [8] Gang Dai, Yifan Zhang, Qingfeng Wang, Qing Du, Zhuliang Yu, Zhuoman Liu, and Shuangping Huang. Disentangling writer and character styles for handwriting generation. In *CVPR*, pages 5977–5986, 2023. 3
- [9] Gang Dai, Yifan Zhang, Quhui Ke, Qiangya Guo, and Shuangping Huang. One-dm: One-shot diffusion mimicker for handwritten text generation. In *ECCV*, pages 410–427, 2024. 3
- [10] Danny Driess, Fei Xia, Mehdi S. M. Sajjadi, Corey Lynch, Aakanksha Chowdhery, Brian Ichter, Ayzaan Wahid, Jonathan Tompson, Quan Vuong, Tianhe Yu, Wenlong Huang, Yevgen Chebotar, Pierre Sermanet, Daniel Duckworth, Sergey Levine, Vincent Vanhoucke, Karol Hausman, Marc Toussaint, Klaus Greff, Andy Zeng, Igor Mordatch, and Pete Florence. Palm-e: An embodied multimodal language model. In *ICML*, pages 8469–8488, 2023. 3
- [11] Yu Du, Fangyun Wei, Ziheng Zhang, Miaoqing Shi, Yue Gao, and Guoqi Li. Learning to prompt for open-vocabulary object detection with vision-language model. In *CVPR*, pages 14064–14073, 2022. 3
- [12] Hao Fei, Shengqiong Wu, Hanwang Zhang, Tat-Seng Chua, and Shuicheng Yan. Vitron: A unified pixel-level vision llm for understanding, generating, segmenting, editing. In *NeurIPS*, 2024. 3
- [13] Tianyu Gao, Adam Fisch, and Danqi Chen. Making pre-trained language models better few-shot learners. In *ACL*, pages 3816–3830, 2021. 3
- [14] Akshay Gopalkrishnan, Ross Greer, and Mohan Trivedi. Multi-frame, lightweight & efficient vision-language models for question answering in autonomous driving. *arXiv preprint arXiv:2403.19838*, 2024. 3, 5, 6
- [15] Wencheng Han, Dongqian Guo, Cheng-Zhong Xu, and Jianbing Shen. Dme-driver: Integrating human decision logic and 3d scene perception in autonomous driving. *CoRR*, abs/2401.03641, 2024. 2
- [16] Edward J. Hu, Yelong Shen, Phillip Wallis, Zeyuan Allen-Zhu, Yuanzhi Li, Shean Wang, Lu Wang, and Weizhu Chen. Lora: Low-rank adaptation of large language models. In *ICLR*, 2022. 4, 5
- [17] Shengding Hu, Yuge Tu, Xu Han, Chaoqun He, Ganqu Cui, Xiang Long, Zhi Zheng, Yewei Fang, Yuxiang Huang, Weilin Zhao, Xinrong Zhang, Zhen Leng Thai, Kai Zhang, Chongyi Wang, Yuan Yao, Chenyang Zhao, Jie Zhou, Jie Cai, Zhongwu Zhai, Ning Ding, Chao Jia, Guoyang Zeng, Dahai Li, Zhiyuan Liu, and Maosong Sun. Minicpm: Unveiling the potential of small language models with scalable training strategies. *CoRR*, abs/2404.06395, 2024. 2
- [18] Haoxu Huang, Fanqi Lin, Yingdong Hu, Shengjie Wang, and Yang Gao. Copa: General robotic manipulation through spatial constraints of parts with foundation models. *CoRR*, abs/2403.08248, 2024. 1, 2
- [19] Yuichi Inoue, Yuki Yada, Kotaro Tanahashi, and Yu Yamaguchi. Nuscenes-mqa: Integrated evaluation of captions and QA for autonomous driving datasets using markup annotations. In *WACV Workshop*, pages 930–938, 2024. 2
- [20] Menglin Jia, Luming Tang, Bor-Chun Chen, Claire Cardie, Serge J. Belongie, Bharath Hariharan, and Ser-Nam Lim. Visual prompt tuning. In *ECCV*, pages 709–727, 2022. 3
- [21] Xiaosong Jia, Yulu Gao, Li Chen, Junchi Yan, Patrick Langechuan Liu, and Hongyang Li. Driveadapter: Breaking the coupling barrier of perception and planning in end-to-end autonomous driving. In *ICCV*, pages 7919–7929, 2023. 3
- [22] Suhyeon Lee, Won Jun Kim, Jinho Chang, and Jong Chul Ye. LLM-CXR: instruction-finetuned LLM for CXR image understanding and generation. In *ICLR*, 2024. 3
- [23] Junnan Li, Dongxu Li, Silvio Savarese, and Steven C. H. Hoi. BLIP-2: bootstrapping language-image pre-training with frozen image encoders and large language models. In *ICML*, 2023. 2
- [24] Yanze Li, Wenhua Zhang, Kai Chen, Yanxin Liu, Pengxiang Li, Ruiyuan Gao, Lanqing Hong, Meng Tian, Xinhai Zhao, Zhenguo Li, Dit-Yan Yeung, Huchuan Lu, and Xu Jia. Automated evaluation of large vision-language models on self-driving corner cases. *CoRR*, abs/2404.10595, 2024. 1, 2, 5
- [25] Zhiqi Li, Wenhai Wang, Hongyang Li, Enze Xie, Chonghao Sima, Tong Lu, Yu Qiao, and Jifeng Dai. Bevformer: Learning bird’s-eye-view representation from multi-camera images via spatiotemporal transformers. In *ECCV*, pages 1–18, 2022. 1

- [26] Chin-Yew Lin. Rouge: A package for automatic evaluation of summaries. *ACL*, 2004. 5
- [27] Haotian Liu, Chunyuan Li, Yuheng Li, and Yong Jae Lee. Improved baselines with visual instruction tuning. In *CVPR*, pages 26286–26296, 2024. 2, 6
- [28] Ilya Loshchilov and Frank Hutter. Decoupled weight decay regularization. In *ICLR*, 2019. 5
- [29] Yingzi Ma, Yulong Cao, Jiachen Sun, Marco Pavone, and Chaowei Xiao. Dolphins: Multimodal language model for driving. *CoRR*, abs/2312.00438, 2023. 1
- [30] Srikanth Malla, Chiho Choi, Isht Dwivedi, Joon Hee Choi, and Jiachen Li. DRAMA: joint risk localization and captioning in driving. In *WACV*, pages 1043–1052, 2023. 2
- [31] Jiageng Mao, Yuxi Qian, Hang Zhao, and Yue Wang. Gpt-driver: Learning to drive with GPT. *CoRR*, abs/2310.01415, 2023. 2
- [32] Juhong Min, Shyamal Buch, Arsha Nagrani, Minsu Cho, and Cordelia Schmid. Morevqa: Exploring modular reasoning models for video question answering. In *CVPR*, pages 13235–13245, 2024. 3
- [33] Soroush Nasiriany, Fei Xia, Wenhao Yu, Ted Xiao, Jacky Liang, Ishita Dasgupta, Annie Xie, Danny Driess, Ayzaan Wahid, Zhuo Xu, Quan Vuong, Tingnan Zhang, Tsang-Wei Edward Lee, Kuang-Huei Lee, Peng Xu, Sean Kirmani, Yuke Zhu, Andy Zeng, Karol Hausman, Nicolas Heess, Chelsea Finn, Sergey Levine, and Brian Ichter. PIVOT: iterative visual prompting elicits actionable knowledge for vlms. In *ICML*, 2024. 2
- [34] Ming Nie, Renyuan Peng, Chunwei Wang, Xinyue Cai, Jianhua Han, Hang Xu, and Li Zhang. Reason2drive: Towards interpretable and chain-based reasoning for autonomous driving. *CoRR*, abs/2312.03661, 2023. 2
- [35] Kishore Papineni, Salim Roukos, Todd Ward, and Wei-Jing Zhu. Bleu: a method for automatic evaluation of machine translation. In *ACL*, pages 311–318, 2002. 5
- [36] Wenjie Peng, Hongxiang Huang, Tianshui Chen, Quhui Ke, Gang Dai, and Shuangping Huang. Globally correlation-aware hard negative generation. *International Journal of Computer Vision*, pages 1–22, 2024. 3
- [37] Tianwen Qian, Jingjing Chen, Linhai Zhuo, Yang Jiao, and Yu-Gang Jiang. Nuscenes-qa: A multi-modal visual question answering benchmark for autonomous driving scenario. In *AAAI*, pages 4542–4550, 2024. 1, 2
- [38] Sheng Shen, Shijia Yang, Tianjun Zhang, Bohan Zhai, Joseph E. Gonzalez, Kurt Keutzer, and Trevor Darrell. Multi-task vision-language prompt tuning. In *WACV*, pages 5644–5655, 2024. 3
- [39] Chonghao Sima, Katrin Renz, Kashyap Chitta, Li Chen, Hanxue Zhang, Chengen Xie, Ping Luo, Andreas Geiger, and Hongyang Li. Drivelm: Driving with graph visual question answering. *CoRR*, abs/2312.14150, 2023. 2, 5, 6, 7
- [40] Ran Tian, Boyi Li, Xinshuo Weng, Yuxiao Chen, Edward Schmerling, Yue Wang, Boris Ivanovic, and Marco Pavone. Tokenize the world into object-level knowledge to address long-tail events in autonomous driving. *CoRR*, abs/2407.00959, 2024. 1, 3
- [41] Xiaoyu Tian, Junru Gu, Bailin Li, Yicheng Liu, Chenxu Hu, Yang Wang, Kun Zhan, Peng Jia, Xianpeng Lang, and Hang Zhao. Drivelm: The convergence of autonomous driving and large vision-language models. *CoRR*, abs/2402.12289, 2024. 1, 2
- [42] Ramakrishna Vedantam, C. Lawrence Zitnick, and Devi Parikh. Cider: Consensus-based image description evaluation. In *CVPR*, pages 4566–4575, 2015. 5
- [43] Shihao Wang, Yingfei Liu, Tiancai Wang, Ying Li, and Xiangyu Zhang. Exploring object-centric temporal modeling for efficient multi-view 3d object detection. In *ICCV*, pages 3598–3608, 2023. 4
- [44] Tianqi Wang, Enze Xie, Ruihang Chu, Zhenguo Li, and Ping Luo. Drivecot: Integrating chain-of-thought reasoning with end-to-end driving. *CoRR*, abs/2403.16996, 2024. 2
- [45] Licheng Wen, Daocheng Fu, Xin Li, Xinyu Cai, Tao Ma, Pinlong Cai, Min Dou, Botian Shi, Liang He, and Yu Qiao. Dilu: A knowledge-driven approach to autonomous driving with large language models. *arXiv preprint arXiv:2309.16292*, 2023. 1
- [46] Chen Henry Wu, Saman Motamed, Shaunak Srivastava, and Fernando De la Torre. Generative visual prompt: Unifying distributional control of pre-trained generative models. In *NeurIPS*, 2022. 3
- [47] Dongming Wu, Wencheng Han, Tiancai Wang, Yingfei Liu, Xiangyu Zhang, and Jianbing Shen. Language prompt for autonomous driving. *CoRR*, abs/2309.04379, 2023. 1
- [48] Jiannan Xiang, Tianhua Tao, Yi Gu, Tianmin Shu, Zirui Wang, Zichao Yang, and Zhiting Hu. Language models meet world models: Embodied experiences enhance language models. In *NeurIPS*, 2023. 1
- [49] Zhenhua Xu, Yujia Zhang, Enze Xie, Zhen Zhao, Yong Guo, Kwan-Yee K. Wong, Zhenguo Li, and Hengshuang Zhao. Drivegpt4: Interpretable end-to-end autonomous driving via large language model. *IEEE Robotics Autom. Lett.*, 9(10): 8186–8193, 2024. 1, 3
- [50] Shiyu Xuan, Qingpei Guo, Ming Yang, and Shiliang Zhang. Pink: Unveiling the power of referential comprehension for multi-modal llms. In *CVPR*, pages 13838–13848, 2024. 2
- [51] Zihui Xue, Kumar Ashutosh, and Kristen Grauman. Learning object state changes in videos: An open-world perspective. In *CVPR*, pages 18493–18503, 2024. 3
- [52] Chenyu Yang, Yuntao Chen, Hao Tian, Chenxin Tao, Xizhou Zhu, Zhaoxiang Zhang, Gao Huang, Hongyang Li, Yu Qiao, Lewei Lu, Jie Zhou, and Jifeng Dai. Bevformer v2: Adapting modern image backbones to bird’s-eye-view recognition via perspective supervision. In *CVPR*, pages 17830–17839, 2023. 1
- [53] Jianwei Yang, Hao Zhang, Feng Li, Xueyan Zou, Chunyuan Li, and Jianfeng Gao. Set-of-mark prompting unleashes extraordinary visual grounding in GPT-4V. *CoRR*, abs/2310.11441, 2023. 2, 3
- [54] Lingfeng Yang, Yueze Wang, Xiang Li, Xinlong Wang, and Jian Yang. Fine-grained visual prompting. In *NeurIPS*, 2023. 3
- [55] Zhenjie Yang, Xiaosong Jia, Hongyang Li, and Junchi Yan. Llm4drive: A survey of large language models for autonomous driving. *CoRR*, abs/2311.01043, 2023. 2

- [56] Runpeng Yu, Weihao Yu, and Xinchao Wang. Attention prompting on image for large vision-language models. *CoRR*, abs/2409.17143, 2024. [3](#)
- [57] Andy Zeng, Maria Attarian, Brian Ichter, Krzysztof Marcin Choromanski, Adrian Wong, Stefan Welker, Federico Tombari, Aweek Purohit, Michael S. Ryoo, Vikas Sindhwani, Johnny Lee, Vincent Vanhoucke, and Pete Florence. Socratic models: Composing zero-shot multimodal reasoning with language. In *ICLR*, 2023. [3](#)
- [58] Enming Zhang, Xingyuan Dai, Yisheng Lv, and Qinghai Miao. Minidrive: More efficient vision-language models with multi-level 2d features as text tokens for autonomous driving. *arXiv preprint arXiv:2409.07267*, 2024. [3](#), [5](#), [6](#)
- [59] Renrui Zhang, Jiaming Han, and Chris Liu et al. LLaMA-adapter: Efficient fine-tuning of large language models with zero-initialized attention. In *ICLR*, 2024. [6](#), [8](#)
- [60] Kaiyang Zhou, Jingkang Yang, Chen Change Loy, and Ziwei Liu. Conditional prompt learning for vision-language models. In *CVPR*, pages 16795–16804, 2022. [3](#)
- [61] Yunsong Zhou, Linyan Huang, Qingwen Bu, Jia Zeng, Tianyu Li, Hang Qiu, Hongzi Zhu, Minyi Guo, Yu Qiao, and Hongyang Li. Embodied understanding of driving scenarios. *arXiv preprint arXiv:2403.04593*, 2024. [1](#), [2](#), [5](#)
- [62] Deyao Zhu, Jun Chen, Xiaoqian Shen, Xiang Li, and Mohamed Elhoseiny. Minigpt-4: Enhancing vision-language understanding with advanced large language models. In *ICLR*, 2024. [1](#), [2](#)

MPDrive: Improving Spatial Understanding with Marker-Based Prompt Learning for Autonomous Driving

Supplementary Material

In this supplementary material, we provide additional details regarding MPDrive and present further ablation studies. Initially, we define the evaluation metrics used to assess performance on the DriveLM dataset. These metrics include accuracy and matching scores. Subsequently, we conducted a series of ablation studies to investigate the effects of different detection experts and image token lengths. For qualitative analysis, we present three types of examples. Firstly, we provide visual prompt comparisons to highlight the differences between MPDrive and InternVL-2. Secondly, ablation examples are included to demonstrate the impact of each component on the generated responses. Finally, we present comparative case studies showcasing the performance differences between MPDrive and InternVL-2.

1. More Evaluation Details

Accuracy Metric For the DriveLM dataset, both multi-choice questions and yes/no questions are used to calculate the accuracy score. The multi-choice questions include perception and behavior prediction. For perception questions, the question is “What is the moving status of the object?”. We will provide 7 candidate options, randomly selecting 3 options from the incorrect answers and incorporating the correct answer to construct the multiple-choice question. Similarly, for behavior prediction questions, the question is “Predict the behavior of the ego vehicle.”, with a total of 21 candidate options. The yes/no questions include perception, prediction, and planning, and the ground truth annotations only contain “yes” or “no”.

Given m predicted responses $\hat{S} = (\hat{r}_1, \hat{r}_2, \dots, \hat{r}_m)$ and the ground truth answers $R = (r_1, r_2, \dots, r_m)$, the accuracy score can be calculated as follows:

$$Acc = \sum_{i=1}^m \frac{\hat{r}_i == r_i}{m}, \quad (4)$$

where $\hat{r}_i == r_i$ is a boolean expression: it equals 1 if the predicted response matches the ground truth, and 0 otherwise.

2. Ablation Study on Different Image Token Lengths

Match Metric For the DriveLM dataset, we extracted l_{gt} center coordinates $P = [p_1, p_2, \dots, p_{l_{gt}}]$ from the ground truth responses and l_p center coordinates $\hat{P} = [\hat{p}_1, \hat{p}_2, \dots, \hat{p}_{l_p}]$ from the predicted responses. We then cal-

culated the proportion of coordinates in the predicted responses that have an Euclidean distance of less than 16 from the ground truth coordinates, thus obtaining the matching ratio, formulated as:

$$Match = \frac{\min(\|P - \hat{P}\|_2) < 16}{l_{gt}}, \quad (5)$$

where $\min(\|P - \hat{P}\|_2) < 16$ represents the number of pairs of points between the P and \hat{P} for which the minimum Euclidean distance is less than 16 among all possible matches.

3. Ablation Study on Different Detection Experts

To investigate the impact of detection expert performance on spatial localization accuracy, we conducted a comparative analysis using two distinct detection models: StreamPetr and DETR3D, which achieve mAP scores of 48.20 and 50.10, respectively, on the NuScenes Val Set, as shown in Table 6. Experimental results indicate a positive correlation between detector performance and spatial localization accuracy. Higher-performing detectors generally exhibit improved spatial localization.

To examine the effect of different image token lengths, we experiment with compressing scene-level tokens from 256 to 64 per image, thereby reducing the total scene tokens from 1,536 to 384 for six view images. As shown in table 5, this token compression strategy led to a degradation in model performance on the DriveLM dataset. Specifically, the decline in accuracy metrics suggests that reducing the number of image tokens compromised the model’s ability to effectively capture and process visual information.

4. Qualitative Visual Prompt Comparison

To demonstrate the effectiveness of our spatial-enhanced features, we conduct a qualitative analysis comparing the visual prompt activation maps between MPDrive and InternVL-2 (Figure 4). While both models exhibit scene awareness for common road elements (e.g., trucks, cars, and traffic signs), InternVL-2 shows notable limitations in object perception, either failing to detect key objects (as shown in the left example where it misses the truck on the road) or displaying redundant activation in non-informative road areas (as illustrated in the right example). In contrast, MP-

Method	Spatial↑ Perception	Language↑				
	Match	Accuracy	BLEU-4	ROUGE.L	CIDEr	METEOR
MPDrvie (64)	13.76	79.37	52.35	76.95	3.54	38.10
MPDrive (256)	13.43	85.18	52.71	76.98	3.56	38.31

Table 5. Ablation study of different image tokens.

Method	mAP	Spatial↑ Perception	Language↑				
		Match	Accuracy	BLEU-4	ROUGE.L	CIDEr	METEOR
MPDrvie (DETR3D)	50.10	13.76	83.30	52.40	76.99	3.58	37.38
MPDrvie (StreamPetr)	48.20	13.43	85.18	52.71	76.98	3.56	38.31

Table 6. Ablation study of different detection experts.

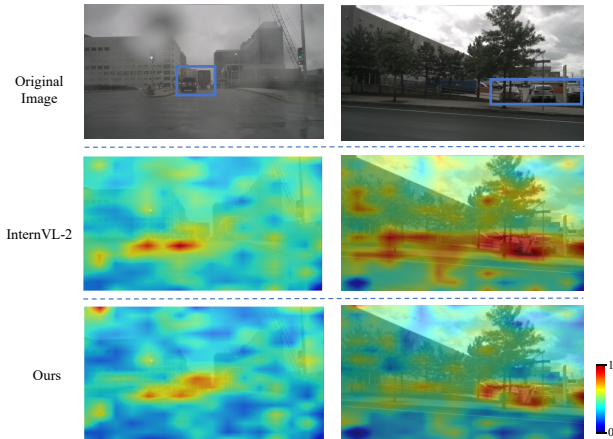


Figure 4. Visual prompt activation examples between InternVL-2 and our proposed MPDrive.

Drive demonstrates more focused and efficient spatial attention by activating only task-relevant vehicles, eliminating redundant information, and maintaining better spatial localization of relevant objects.

5. Qualitative Ablation Examples

Figure 5 demonstrates the impact of different components of MPDrive on the responses, we display the predicted coordinates from one of the most relevant images, and after introducing the Visual Marker, the predicted coordinates contain one correct answer. Following the incorporation of MCNet, the model output multiple coordinates in the front-view image, all of which were located on objects; however, the answer included irrelevant objects such as barriers and trucks. With the addition of the instance-level visual prompt, the model was able to locate each coordinate accurately. This sample indicates that the Visual Marker and MCNet contribute to the precise representation of the spa-

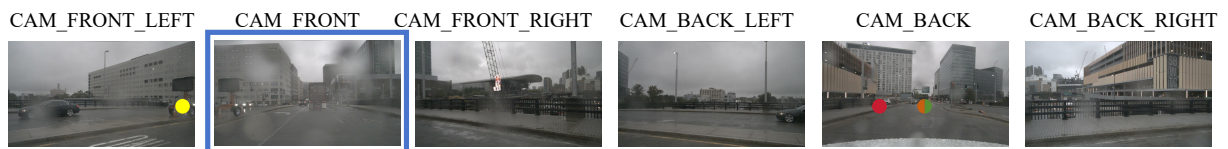
tial coordinates of objects, ensuring consistency in language expression. Meanwhile, the instance-level prompt enhances the spatial features of the objects, further improving the spatial perception capabilities of MPDrive.

6. More Qualitative Examples

In this section, we present more qualitative examples of MPDrive responses. Figure 6 illustrates a comparison between the response results of MPDrive and InternVL-2. In the first sample of Figure 6, for the question of identifying whether the mentioned pedestrian is an important object, InternVL-2 incorrectly answers that the pedestrian crossing the street is not an object that should be considered, however, the pedestrian on the left side is indeed significant because the ego vehicle is making a left turn, and MPDrive provides an accurate assessment in this scenario. Similarly, in the second sample, for the question of understanding the relationship between the mentioned vehicle and the traffic light, InternVL-2 incorrectly assumes that the car is unrelated to the traffic light. However, the traffic light signals influence the vehicle’s position. MPDrive, with its excellent spatial perception abilities, can accurately recognize the relationship between the car and the traffic light. In the last two samples, for the questions of identifying the dangerous behaviors between the ego vehicle and other vehicles, InternVL-2 struggles to recognize the relative spatial relationships between the ego vehicle and the relevant vehicles due to a lack of strong spatial perception capabilities, thereby limiting its ability to identify potential dangerous behaviors accurately. In contrast, MPDrive successfully perceives the spatial positions of the relevant vehicles, because of its superior spatial perception abilities, allowing it to make accurate planning decisions.

In summary, MPDrive demonstrates an advantage in scenarios requiring precise spatial perception. Its ability to accurately interpret spatial relationships and identify critical

objects allows it to make more informed and safer planning decisions. This enhanced spatial understanding is crucial for the effective navigation and safety of autonomous systems, highlighting the potential of MPDrive for superior performance in complex driving environments.



Q: What is the priority of the objects that the ego vehicle should consider?(in descending order) ?

GT: <c1,CAM_FRONT_LEFT,1495.7,474.1>,
<c3,CAM_FRONT,905.0,448.3>, <c2,CAM_FRONT,761.7,528.3>.

Visual Marker: The priority of the objects that the ego vehicle should consider (in descending order) is <c1,CAM_FRONT,873.0,441.0>,
<c2,CAM_BACK,810.0,512.0>.

Visual Marker+MCNet: The priority of the objects that the ego vehicle should consider (in descending order) is <c1,CAM_FRONT,873.0,441.0>,
<c4,CAM_FRONT,163.0,460.0>, <c3,CAM_FRONT,78.0,619.0>,
<c2,CAM_BACK,459.0,509.0>.

MPDrive: The priority of the objects that the ego vehicle should consider (in descending order) is <c1,CAM_FRONT,873.0,441.0>,
<c2,CAM_FRONT,764.0,517.0>, <c3,CAM_BACK,810.0,512.0>.

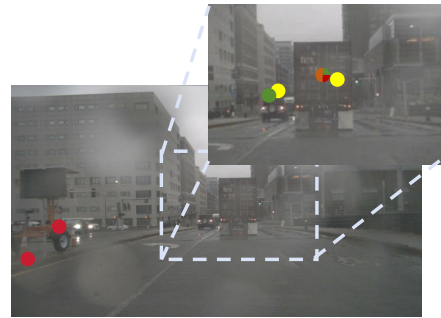


Figure 5. Comparison of different components of MPDrive on the responses. The yellow (■) area and dots represent the response and coordinates of ground truth (GT), the brown (■) area and dots indicate the response and coordinates after adding the Visual Marker, the red (■) area and dots denote the response and coordinates after adding the Visual Marker and the MCNet, and the green (■) area and dots indicate the response and coordinates of MPDrive.



Q: Is $\langle c1, CAM_FRONT, 455.8, 508.3 \rangle$ an object that the ego vehicle should consider in the current scene?

GT: Yes.

InternVL2: No.

MPDrive: Yes.

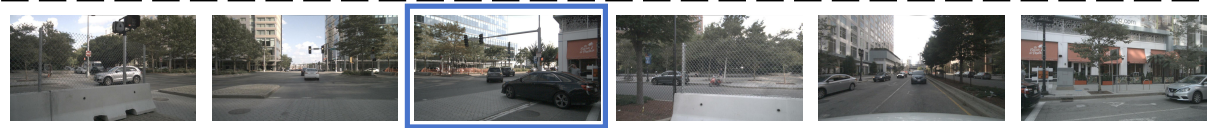
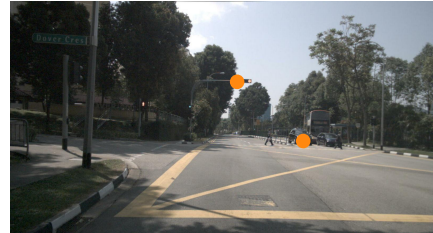


Q: Would $\langle c4, CAM_FRONT, 1091.7, 509.2 \rangle$ take $\langle c6, CAM_FRONT, 900.2, 294.8 \rangle$ into account?

GT: Yes.

InternVL2: No.

MPDrive: Yes.

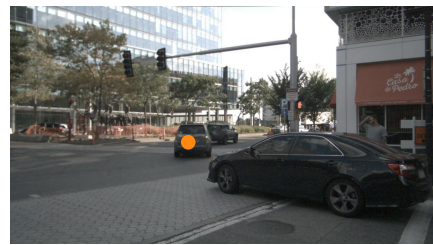


Q: What actions taken by the ego vehicle can lead to a collision with $\langle c3, CAM_FRONT_RIGHT, 647.7, 510.0 \rangle$?

GT: Sharp right turn.

InternVL2: No action taken by the ego vehicle will lead to a collision with $\langle c3, CAM_FRONT_RIGHT, 647.7, 510.0 \rangle$.

MPDrive: Sharp right turn.



Q: What actions taken by the ego vehicle can lead to a collision with $\langle c4, CAM_FRONT, 367.5, 515.8 \rangle$?

GT: Sharp right turn.

InternVL2: No action taken by the ego vehicle will lead to a collision with $\langle c4, CAM_FRONT_RIGHT, 367.5, 515.8 \rangle$.

MPDrive: Sharp right turn.

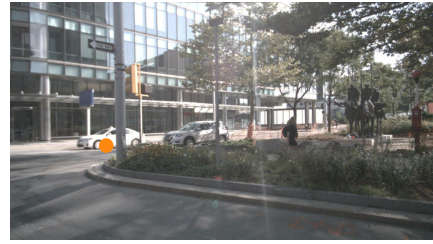


Figure 6. Comparison of the responses between InternVL-2 and our proposed MPDrive.